JOURNAL OF ENDODONTICS
Printed in U.S.A.
VOL. 29, NO. 1, JANUARY 2003

Comparative Analysis of Torsional and Bending Stresses in Two Mathematical Models of Nickel-Titanium Rotary Instruments: ProTaper versus ProFile

Elio Berutti, MD, DDS, Giorgio Chiandussi, D Eng, PhD, Ivan Gaviglio, D Eng, and Andrea Ibba, D Eng

During root canal instrumentation, nickel-titanium rotary instruments are subjected to continual stresses inside the canal due to its anatomy and the hardness of the dentin they must cut. They must therefore be both stress-resistant and elastic.

This study aimed to compare the mechanical behavior of two nickel-titanium rotary instruments (ProTaper and ProFile) by applying the finite element analysis method to produce a numerical evaluation.

The nonlinear mechanical behavior of the alloy was taken into account during the study. The distribution of stresses due to torsional and bending moments was compared in the two experimental models. The ProFile model was found to be more elastic than the ProTaper model. Under equal loads, the ProTaper model showed lower and better distributed stresses than the ProFile model.

The introduction of nickel-titanium alloy for the manufacture of mechanically driven endodontic instruments has greatly simplified shaping root canal systems. These instruments are two to three times more flexible than stainless steel instruments (1) and are also markedly superior to stainless steel instruments in terms of angular deflection and maximum torque to failure (2). These two properties—elasticity and strength—gave rise to mechanically driven nickel-titanium engine instruments. These new instruments have been found to be better than stainless steel instruments in maintaining the original anatomy and the shape and position in space of the apical foramen (3, 4).

The stresses to which a nickel-titanium, mechanically driven engine instrument is subjected are completely different than the stresses a manual instrument undergoes. The nickel-titanium, mechanically driven engine instrument is in continuous rotation and thus undergoes unidirectional torque. This subjects the instrument to a constant and variable strain depending on the canal anatomy and the hardness of the dentin to be cut (5). It is therefore of determinant importance to manufacture instruments that are elastic but also strong; the instrument cross-section is very important, because it directly determines torsional and bending properties (6). In analyzing the different nickel-titanium, mechanically driven engine instruments, the cross-section must be considered because it strongly influences the mechanical properties.

This research aimed to compared torsional and bending stresses in two theoretical cross-sections: convex (section A, ProTaper) and concave (section B, ProFile). These two cross-sections were chosen, because chronologically, they reflect the evolution of the nickel-titanium, mechanically driven engine instruments manufactured by Dentsply/Maillefer (Tulsa, OK).

Analysis of the two cross-sections concerned the:

- Geometrical properties of the two cross-sections;
- Mechanical behavior through the two models determined by the finite element method.

MATERIALS AND METHODS

Geometrical Model and Constituent Material

The endodontic instruments analyzed (ProFile and ProTaper) are both characterized by a cross-section with three axes of symmetry, rotated by 120 degrees one from the other, and passing through the barycentre. Both cross-sections are described within a circumference of diameter of 4 mm. The geometrical characteristics of the two cross-sections are given in Fig. 1. The axis perpendicular to the plane of the cross-section was taken as the z axis. The two orthogonal x and y axes lie in the plane of the cross-section. The area, the perimeter, and the moments of inertia about the x, y, and z axes of both cross-sections were calculated and are reported in Table 1.

The material from which the files are made is a nickel-titanium alloy whose mechanical behavior is highly nonlinear. The characteristics of the material are summed up in the graph of stress against strain shown in Fig. 2. The characteristic curve of the material may be subdivided into three parts: the first part is linear, in which the alloy is in a more stable crystalline phase, of the austenitic type; the second part of the graph is also linear but

TABLE 1. Geometric properties of the cross-sections of the endodontic instruments analyzed

Geometric Properties of the Cross-sections	ProTaper (A)	ProFile (B)
Area	0.09086 mm^2	0.06749 mm^2
Perimeter	1.107 mm	1.159 mm
Bending moment of inertia around the x axis	6.738 10^{-4} mm^{-4}	4.508 10^{-4} mm^{-4}
Bending moment of inertia around the y axis	6.738 10^{-4} mm^{-4}	4.508 10^{-4} mm^{-4}
Torsional moment of inertia around the z axis	13.476 10^{-4} mm^{-4}	9.016 10^{-4} mm^{-4}

almost flat, during which the material is in transition from the austenitic to the martensitic phase; the third part of the graph is highly nonlinear, in which the alloy is characterized by a martensitic type phase. The last part of the graph has the typical characteristics of a stress-strain diagram for a metal, with an elastic zone, a yield point, and a breaking point. The second part of the curve describes behavior specific to the material analyzed: a very small stress produces a large strain. This characteristic of the material is generally identified as super-elasticity.

Discrete Model of the Geometry and Behavior of the Material

The mechanical behavior of the two endodontic instruments was analyzed numerically by applying the finite-element method. This method requires a discrete model to be defined of the structure to be analyzed and of the mechanical characteristics of the constituent material; the surrounding conditions must also be fixed (force, moments, and geometrical restrictions) (7, 8).

The mechanical behavior of the instruments with the cross-sections in Fig. 1 may only be compared if the corresponding geometrical models are similar. Both geometric models were therefore made by rotating the characteristic cross-section through 360 degrees over a length 1 = 1.8 mm, equal to the pitch of the helix, measured on the actual instruments. The two models were thus inscribed within cylinders of equal diameter and length. This procedure implicitly ignored the taper of files in general use. The geometric models thus obtained were manually divided into discrete hexahedral elements (Fig. 3). The total number of elements was 3600 for the ProFile model and 3750 for the ProTaper model. In both cases, the model was blocked at one end and was loaded with a concentrated torsional or bending moment at the other end.

The nonlinear behavior of the material was also approximated: the stress-strain curve was simplified to three lines having Young's modulus respectively of 35,700, 860, and 11,600 MPa (Fig. 2).

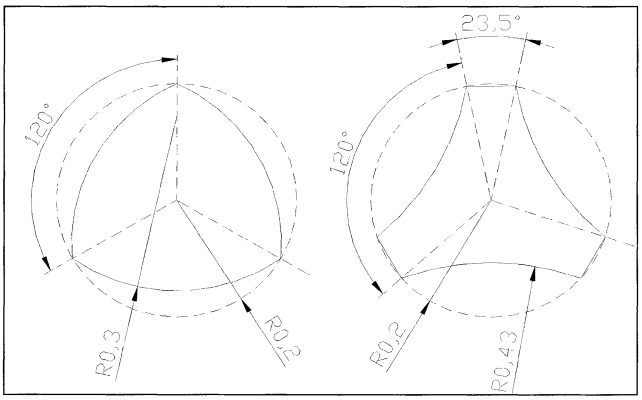

FIG 1. Geometry of the cross-sections of the two endodontic instruments analyzed: ProTaper (*left*); ProFile (*right*).

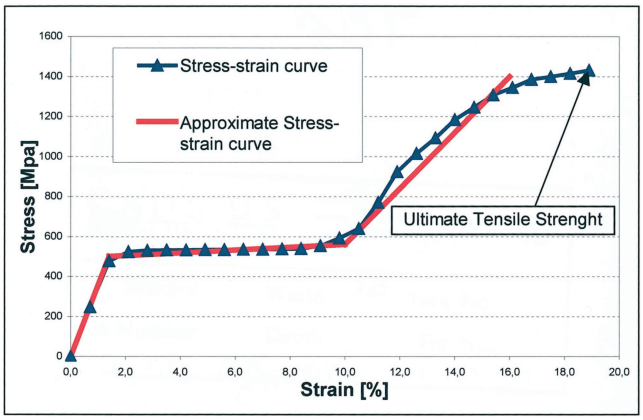

FIG 2. Characteristic graph of the material and its approximation into three linear sections.

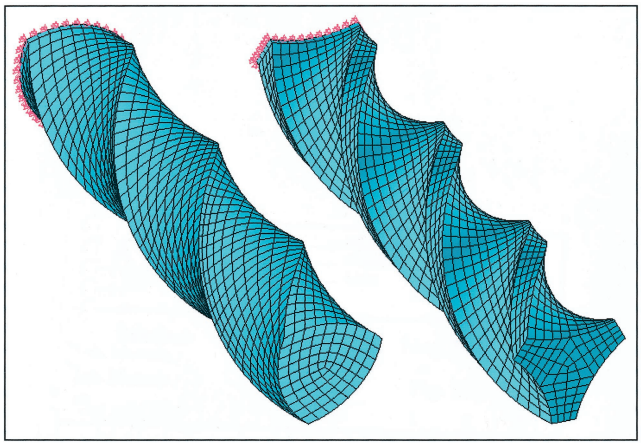

FIG 3. Discrete models used to analyze the instruments with the finite element method: ProTaper model (*left*); ProFile model (*right*).

These nonlinear characteristics of the material mean that the structural rigidity varies in a nonlinear fashion as the applied load varies. Determination of the characteristic bending or torsional rigidity therefore requires a number of analyses to be performed for different applied loads. The characteristic bending rigidity was determined by varying the applied moment between 0 and 4.5 N/mm. The characteristic torsional rigidity was analyzed by varying the applied moment between 0 and 2.5 N/mm.

RESULTS

The following two paragraphs report the results of the analyses made by applying a concentrated torsional or bending moment to the above models. The analyses do not take into account the forces applied to the two models by any external structure (dentin).

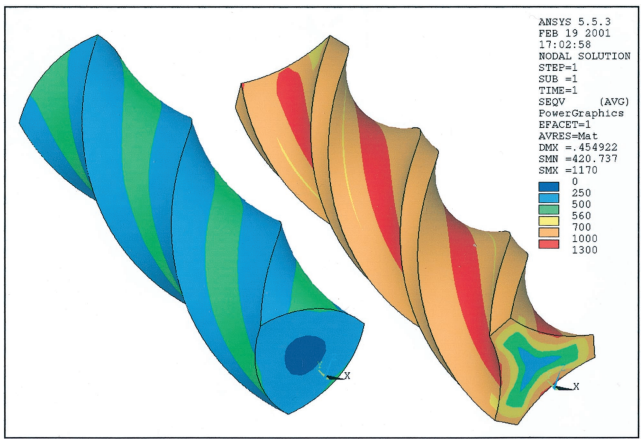

FIG 4. Distribution of von Mises stresses with an applied torsional moment of 2.5 N/mm.

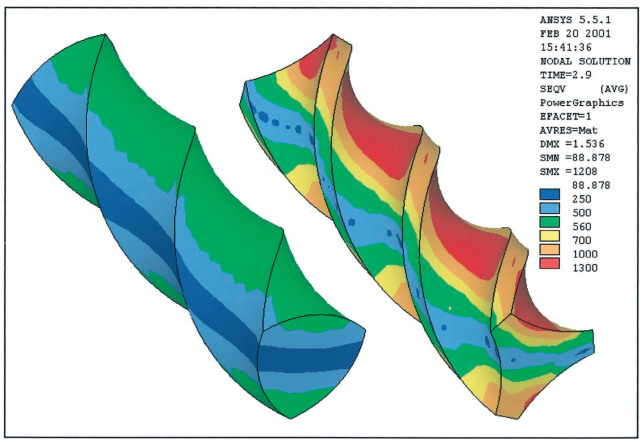

FIG 5. Distribution of von Mises stresses with an applied bending moment of 2.9 N/mm.

Torsional Behavior

Figure 4 shows the distribution of Von Mises stresses obtained by applying a torsional moment of 2.5 N/mm to both models. In both cases, stress values increase radially outwards from the center of the model, where the neutral stress axis lies. The distribution of stresses in the model with the ProTaper cross-section is more regular and uniform. The model with the ProFile cross-section has marked stress peaks along the flutes and higher maximum stress values.

The central core of both models is subjected to less stress, with values between 0 and 500 N/mm^2 (Fig. 4, blue/light blue). In this area, the material is entirely in the austenitic phase. The external part of the models, on the contrary, operates in the super-elastic field with stress values between approximately 500 and 560 N/mm^2 (Fig. 4, green). In this case, the material is characterized by the simultaneous presence of an austenitic phase and a martensitic phase. In the case of the model with the ProFile section, the most external portion of material is subject to stress values above 560 N/mm^2 (Fig. 4, yellow/red). In this area, the material is in the martensitic phase and has lost the characteristic of super-elasticity.

Behavior at Bending

Figure 5 shows the distribution of Von Mises stresses obtained by applying a bending moment of 2.9 N/mm^2 to both models. In both cases, stress values increase as the distance from the neutral bending plane increases. These stresses may be of the traction or the compression type, depending on the position with respect to the neutral plane. The applied bending moment being equal, the model with the ProTaper section once again has lower maximum stress values. The central part of the model is characterized by stress values between 0 and 500 N/mm^2 (Fig. 5, blue/light blue); here, the material is in the austenitic phase. Proceeding toward the outer part of the models, an area may be seen with stress values between 500 and 560 N/mm^2 (Fig. 5, green), where the material is characterized by the contemporary presence of the austenitic and martensitic phases and by super-elastic behavior; there is also an area with stress values above 560 N/mm^2, in which the material is characterized by a fully martensitic phase (Fig. 5, yellow/red).

Figure 6 shows the distribution of Von Mises stresses on three different cross-sections of the two models subjected to a constant bending moment. Some instability may be seen in the area of material with low stress values, close to the neutral stress plane. It is also interesting to note that, in the model with the ProFile section, the maximum stress value is found to correspond with the flutes between the blades and not in the area most distant from the neutral stress plane. This stress peak varies in position within the flutes as the position of the cross-section varies.

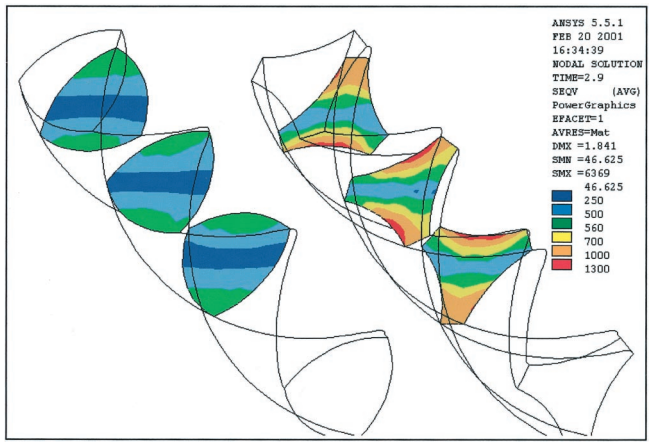

FIG 6. Distribution of von Mises stresses in three different cross-sections with an applied bending moment of 2.9 N/mm.

Characteristic Rigidity Curves

The static bending and torsional rigidity of the models analyzed is not constant as the applied load varies. It depends on the crystalline phase of the material in the different parts of the model and thus on the stress and strain conditions generated by the applied load.

Comparison between the characteristic rigidity curves of the two models analyzed leads to some further considerations. Figure 7 shows an example of characteristic bending rigidity curves. The first part of the two curves is practically horizontal. The material of the cross-section of both models is in the austenitic phase. The displacement of the moment applied varies linearly with the load, and bending rigidity thus remains constant. In this part of the curve, the difference in rigidity between the two models is only due

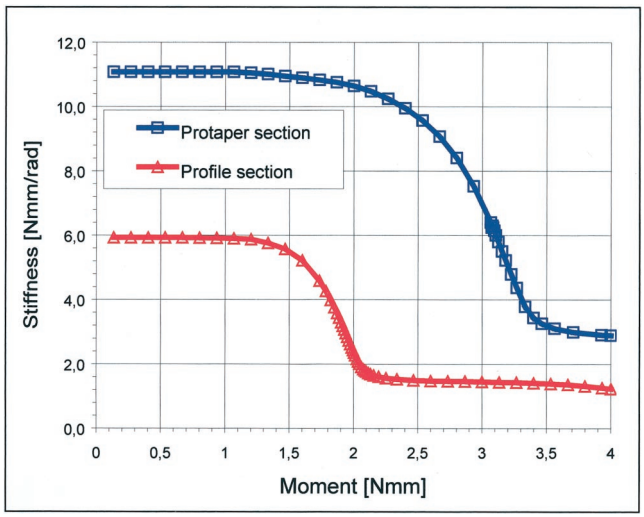

FIG 7. Characteristic curve of bending rigidity for the two discrete models analyzed.

to the different moment of inertia of the two cross-sections. The model with the ProTaper section is that which, external diameters being equal, has the higher moment of inertia and thus the greater bending rigidity.

Increasing the applied bending moment, the material of the more external part of the cross-section of the models is subjected to stress values typical of the transition between austenitic and martensitic phases. This material behaves in a super-elastic fashion, and the bending rigidity of the two models varies as the proportion of material in the super- elastic field varies. The different behavior of the two models is, in this case, due to the different geometry of the cross-sections (curved portion of the graph).

The bending rigidity tends to become almost constant again when most of the material is in the martensitic phase. The different bending rigidity values of the two models is again chiefly due to the different moments of inertia of the two cross-sections. In this case, too, the characteristic curves may be subdivided into three parts. The central part identifies the presence of material in transition from the austenitic to the martensitic phase. The transition from the first part of the curve, characterized by a constant rigidity value, to the third part of the curve, also characterized by almost constant rigidity, occurs much more rapidly in the case of the model with the ProFile section. The portion of material operating in the super-elastic field is in this case very rapidly reduced as the applied load increases. In the case of the model with the ProTaper cross-section, on the contrary, this transition phase is much more gradual and interprets a more gradual change of the material from the austenitic to the martensitic phase as the applied load increases. The model with the ProTaper cross-section is thus characterized by the presence of an extensive super-elastic zone for a much wider range of applied loads than occurs with the ProFile section.

DISCUSSION

This research analyses the different mechanical behavior of the cross-sections of two nickel-titanium, mechanically driven engine instruments, ProTaper and ProFile. The research takes into account the highly nonlinear mechanical behavior of the nickel-titanium alloy from which the two instruments are made (9–11). This is of fundamental importance, because in producing these mechanically driven engine instruments, two vital characteristics are necessary for success: strength and elasticity (1, 12).

Observing the characteristics of the nickel titanium alloy by analyzing the stress-strain diagram, it may be seen that the highest performance zone for working with nickel-titanium, mechanically driven engine instruments corresponds to the second portion of the diagram, in which a transition occurs from the more stable austenitic crystalline phase to the third portion, representing the martensitic phase, in which the alloy undergoes serious strain, culminating first in yielding and then breaking (13, 14). The second part of the graph represents the so-called transition phase, where super-elastic characteristics occur without any significant increase in stress. It is intuitively obvious that the more the alloy works in this phase, the more elasticity combined with strength it will show (15). The endodontic instrument may thus shape the root canal, following the original canal anatomy however complex it may be, without reaching and accumulating high stress values (16, 17).

The two cross-sections, although both lie within a circumference of diameter 0.4 mm, have markedly different geometrical properties. Section A (ProTaper) has an area almost 30% greater than section B (ProFile). This means that the ProFile has less mass and thus a significantly lower moment of inertia, making it more elastic than the ProTaper.

The intensity and distribution of the stresses on each model after application of first, a torsional moment, and second, a bending moment, were also analyzed. A bending moment occurs, and in consequence bending stresses, each time the continually rotating instrument meets resistance (dentin) that acting on the more external surface (blades) blocks this rotation to a greater or lesser extent. It might be said that this is the principle by which the dentin can be cut, but in extreme cases, when the resistance is so high as to block the instrument, the instrument itself breaks.

Distribution of stresses in the model with the ProTaper cross-section was regular and uniform, whereas in the model with the ProFile section there were high tension peaks in the flutes between the blades and a less regular distribution.

The intensity of the stresses is also more favorable in the model with the ProTaper cross-section, which in the more superficial portions, operates in the super-elastic field (transformation phase). The model with the ProFile cross-section, on the contrary, reaches very high stresses concentrated in the flutes between the blades where the material loses the super-elastic characteristic, having reached the martensitic phase. It thus seems clears that in the ProTaper model stresses are less intense and are more uniformly distributed. In the ProFile model, the accumulation of high stresses concentrated in the flutes between the blades concentrates fatigue in these areas and may create areas of least resistance (18).

The same considerations may be made when a bending moment occurs. When bending occurs, a neutral central bending plane may be determined where, theoretically, there is no stress; the two areas on either side of this plane undergo traction and compression, respectively. Both types of stress increase from the central neutral plane to the external surface of the model, where they reach peak intensity. Also when a bending moment occurs, analysis of the stresses in the two models show that, loads being equal, the ProTaper model undergoes lower stresses, which are distributed more uniformly over the surface than in the ProFile model, which again shows higher stress values concentrated in the flutes between the blades. If we observe the distribution of the stresses on several cross-sections of the models as a bending moment is applied, it is

interesting to note that the neutral bending plane (blue) remains practically constant in the ProTaper model, whereas it is more variable in position in the ProFile model. The stresses are also more uniformly distributed in the ProTaper model than in the ProFile model.

This is important if we consider that nickel-titanium, mechanically driven engine instruments, when working in a curved canal, are in continual rotation, and this causes an alteration of compression and traction stresses in the same cross-section. It is therefore important to have a uniform distribution of stresses to avoid creating stress accumulation zones and thus areas of least resistance (19).

To avoid excessive stress, it is also important that the dentist does not stop with the instrument rotating in a curve of the canal but rather that he/she, with a fluid movement, moves it first apically and then having completed the movement retracts it (20). This enables the cross-section of the instrument corresponding to the apex of the curve (that under the most stress) to change continually, distributing the stresses optimally.

The stresses that are generated in the models analyzed, during a torsional or bending moment, are not constant but vary with the applied load. Indeed, they vary in relation to the crystalline phases of the alloy, which as we saw does not have a linear behavior. Comparing the bending rigidity graphs of the two models, the three crystalline phases characteristic of the alloy may be recognized: the first horizontal phase corresponds to the austenitic phase. The horizontal part of the graph (austenitic phase) is located lower in the ProFile model, because as was said above, the geometric characteristics of its cross-section make it more elastic.

The different behavior of the two models in the subsequent phase, that of phase transformation, is very interesting; this phase is optimal for working with mechanically driven instruments, giving them the characteristic of super-elasticity without excessive stress. The ProFile model moves rapidly from the austenitic phase to the martensitic phase; the transformation phase is in this case short, and the change from the austenitic phase to the martensitic phase is very swift. The behavior of the ProTaper model is different, because the changeover from the austenitic phase to the martensitic phase is gentle and the part of the graph corresponding to this transformation is very long. This means that, applied loads being equal, the ProTaper model works for a longer time in the super-elastic phase (transformation phase), which as we have seen, gives highest performance and is less risky. On the contrary, the ProFile is more elastic but accumulates dangerous stress more rapidly, because the transformation phase is so short that the model frequently has to operate in the martensitic phase.

We conclude the following.

1. The ProFile model (section B) is more elastic than the ProTaper model (section A).
2. The ProFile model (section B) has a very short super-elastic transformation phase. It rapidly reaches the martensitic phase where it accumulates dangerous stress.
3. The ProTaper model (section A) has a very long transformation phase, and thus can operate even with high loads in the transformation phase (super-elastic) without accumulating dangerous stresses.
4. The ProTaper model (section A), being stronger and less elastic, might be more indicated for thin mechanically driven instruments specific for narrow canals and curved canals during the initial phase of shaping.
5. The ProFile model (section B), being more elastic but not so strong, might be more indicated for wider canals and curved canals in the final phase of shaping.
6. The ideal instrument should have both characteristics: elasticity and strength. One solution might be to have mechanical instruments whose cross-section varies along their length.

Dr. Berutti is professor of endodontics, School of Dentistry, Turin University, Turin, Italy. Dr. Chiandussi is assistant professor, and Drs. Gaviglio and Ibba are research assistants, Turin Polytechnic, Turin University, Turin, Italy. Address requests for reprints to Prof. Elio Berutti, Via Susa 37, 10138, Torino, Italy.

References

1. Walia H, Brantley WA, Gerstein H. An initial investigation of the bending and torsional properties of Nitinol root canal files. J Endodon 1988;14:346–51.
2. Camps JJ, Pertot WJ. Torsional and stiffness properties of nickel-titanium K-files. Int Endod J 1995;28:239–43.
3. Glosson CR, Hallor RH, Dove SB, del Rio CE. A comparison of root canal preparations using Ni-Ti hand, Ni-Ti engine driven and K-Flex endodontic instruments. J Endodon 1995;21:146–51.
4. Schäfer E. Root canal instruments for manual use: a review. Endod Dent Traumatol 1997;13:51–64.
5. Serene TP, Adams JD, Saxena A. Nickel-titanium instruments applications in endodontics. St. Louis: Ishiyaku EuroAmerica, 1995.
6. Camps JJ, Pertot WJ, Levallois B. Relationship between file size and stiffness of nickel titanium instruments. Endod Dent Traumatol 1995;11:270–3.
7. Zienkiewicz OC, Taylor RL. The finite element method. London: McGraw-Hill, 1989.
8. Bathe KJ. Finite element procedures. Englewood Cliffs: Prentice-Hall, 1996.
9. Wang FE, Pickart SJ, Alperia HA. Mechanism of the TiNi martensitic transformation and the crystal structures of TiNi-II and TiNi-III phases. J Appl Phys 1972;43:97–112.
10. Otsuka K, Shimuzi K. Pseudoelasticity and shape memory effects in alloy. Int Met Rev 1986;31:93–114.
11. Wayman CM. Shape memory alloys. Materials Res Soc Bull 1993;18: 49–56.
12. Walia H, Costas J, Brantley W, Gerstein H. Torsional ductility and cutting efficiency of the Nitinol file [Abstract]. J Endodon 1989;15:174.
13. Andreasen GF, Morrow RE. Laboratory and clinical analyses of Nitinol wire. Am J Orthod 1978;73:142–51.
14. Thompson SA. An overview of nickel-titanium alloys used in dentistry. Int Endod J 2000;33:297–310.
15. Hodgson DE, Wu MH, Bierman RJ. Shape memory alloys. In: Davis JR, ed. Metals handbook. vol. 2, Properties and selection: nonferrous alloys and special-purpose materials. Materials Park, OH: ASM International, 1990.
16. Kavanagh D, Lumley PJ. An in vitro evaluation of canal preparations using ProFile 0.04 and 0.06 taper instruments. Endod Dent Traumatol 1998; 14:16–20.
17. Bryant ST, Dummer PMH, Pitoni C, Bourba M, Moghal S. Shaping ability of .04 and .06 taper ProFile rotary nickel-titanium instruments in simulated root canal. Int Endod J 1999;32:155–64.
18. Turpin YL, Chagneau F, Vulcain JM. Impact of two theoretical cross-sections on torsional and bending stresses of nickel-titanium root canal instrument models. J Endodon 2000;26:414–7.
19. Turpin YL, Chagneau F, Bartier O, Cathelimeau G, Vulcain JM. Impact of torsional and bending inertia on root canal instruments. J Endodon 2001; 27:333–6.
20. Machtou P, Martin D. Utilisation raisonnée des ProFile. Clinic 1997; 18:253–9.